Direct Polymerization of Highly Polar Acetylene Derivatives and Facile Fabrication of Nanoparticle-Decorated Carbon Nanotubes

Wang Zhang Yuan,[†,‡] Li Tang,[†] Hui Zhao,[†] Jia Ke Jin,[†] Jing Zhi Sun,*[,†] Anjun Qin,[†,‡] Hai Peng Xu,[†] Jiahao Liu,[§] Feng Yang,[†] Qiang Zheng,[†] Erqiang Chen,[§] and Ben Zhong Tang*[,†,‡]

Department of Polymer Science and Engineering, Institute of Biological and Medical Macromolecules, Key Laboratory of Macromolecular Synthesis and Functionalization (Ministry of Education of the Chinese Government), Zhejiang University, Hangzhou 310027, China, Department of Chemistry, Nanoscience and Nanotechnology Program, The Hong Kong University of Science & Technology (HKUST), Clear Water Bay, Kowloon, Hong Kong, China, and Department of Polymer Science and Engineering, College of Chemistry and Molecular Engineering, Peking University, Beijing 100871, China

Received August 31, 2008; Revised Manuscript Received November 18, 2008

ABSTRACT: Acetylenic monomers containing highly polar functional groups, especially those with active hydrogen atoms, have been difficult to polymerize because their toxic interactions with transition metal complexes deactivate catalyst systems. In this work, we succeeded in direct polymerizations of a series of highly polar phenylacetylene derivatives. The polymerizations of 4-ethynylbenzoic acid (**1**), 4-hydroxybutyl 4-ethynylbenzoate (**2**), 6-(4-ethynylphenoxy)hexanoic acid (**3**), 4-ethynylaniline (**4**), and 1-ethynyl-4-nitrobenzene (**5**) catalyzed by organorhodium complexes afforded corresponding polymers (P**1**−P**5**) of high molecular weight (M_w as high as 488 500) and low polydispersity index (M_w/M_n as low as 1.03). The structures of the polymers were characterized spectroscopically. Treatments by base and acid readily transformed neutral polymers P**1** and P**4** to polyelectrolytes P**1**$^-$ and P**4**$^+$, respectively. Simple mixing of the conjugated polyelectrolytes with multiwalled carbon nanotubes (MWNTs) afforded polyacetylene/MWNT nanohybrids with water solubility of up to 316 mg/L. The hybrids were facilely decorated by metal (oxide) nanoparticles, furnishing multicomponent composites of P**1**$^-$/MWNT/Ag, P**4**$^+$/MWNT/Ag, and P**4**$^+$/MWNT/ZnO.

Introduction

Polyacetylenes carrying functionalized pendants have attracted considerable attention because of their potential applications in optoelectronics, biomaterials, enantioseparation, and so forth.[1] The polymers have been found to exhibit diverse functional properties, including mesomorphism,[2] luminescence,[1] photoconductivity,[3] redox activity,[4] gas permeability,[5] chain helicity,[6] and cytophilicity.[7] The past decades have witnessed fast development in the area of functional polyacetylene research,[1] with intense efforts devoted to the synthesis of substituted polyacetylenes with functional groups,[8] the development of effective catalyst systems,[9] and the fabrication of functional polyacetylene-based hybrids.[4,10,11]

The syntheses of functionalized polyacetylenes are critically dependent on the exploration of effective catalysts. Several transition-metal salts and complexes have been found to work as catalysts for the polymerizations of substituted acetylenes.[1] Among them, $NbCl_5$ and $TaCl_5$ salts are effective for only nonpolar acetylenic monomers.[12] Although WCl_6 and $MoCl_5$ are somewhat functionality-tolerant, they are very sensitive to air and moisture and are intolerant of polar functionalities, especially those with active hydrogen atoms, such as amino and amido groups. Metal carbonyl complexes are more stable than the metal halides but need to be preactivated by chlorine-containing additives or UV photoirradiation in halogenated solvents. We have found that a series of $M(CO)_xL_y$ (M: Mo, W; L: ligand) complexes are air- and moisture-stable and work well as catalysts for acetylene polymerization in nonhalogenated solvents.[13] The monomers that can be polymerized by these complexes, however, are limited.

The main obstacle in the polymerizations of the functionalized acetylenes has been the incompatibility of the polar groups in the monomers with the early transition metals in the metathesis catalysts.[1] The discovery of the organorhodium catalysts, which polymerize the acetylenic monomers via an addition instead of a metathesis mechanism, is a milestone in the area of polyacetylene research. The rhodium catalysts can efficiently polymerize various monosubstituted acetylenes, including phenylacetylene and 1-alkynes derivatives with polar groups, to give polymers with high molecular weights and stereoregular Z-s-E conformation.[9,14] Even by using the Rh catalysts, the polymerization of highly polar monomers, particularly those with acidic protons, is still a difficult proposition. For example, the polymerization of acetylenic monomers containing carboxy groups has been a daunting job.[15,16] The direct polymerization of 4-ethynylbenzoic acid (**1**) was deemed very difficult, if not impossible (Scheme 1).

Another example is the synthesis of amino-acid-containing polyacetylenes, which was accomplished through indirect synthetic routes.[17] As shown in Scheme 2, the polymers are prepared in the following way: the carboxy groups of the monomers are protected by esterification with methanol, and

Scheme 1

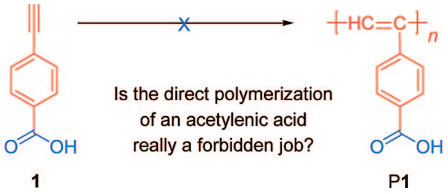

---

* Corresponding authors. E-mail: sunjz@zju.edu.cn (J.Z.S.); tangbenz@ust.hk (B.Z.T.).
[†] Zhejiang University.
[‡] HKUST.
[§] Peking University.

10.1021/ma801978x CCC: $40.75

Scheme 2

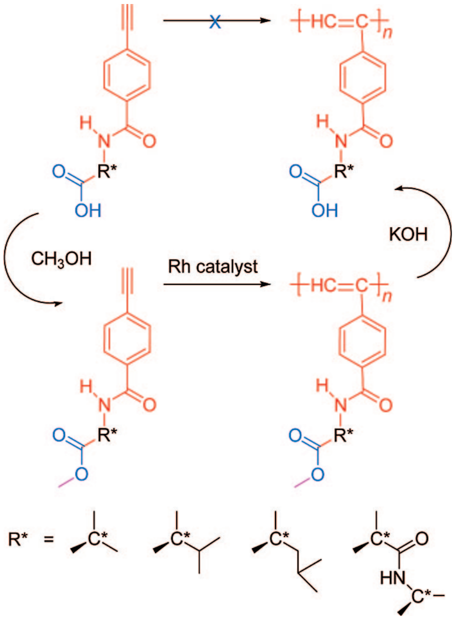

Scheme 3

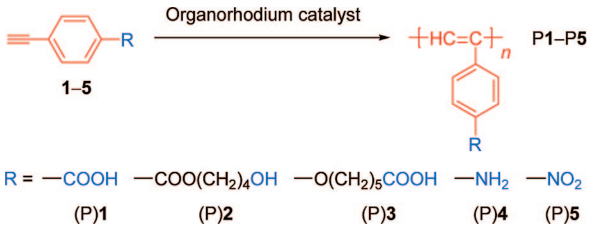

the esters are transformed to polyesters, followed by the base-catalyzed hydrolysis deprotection.[17] Although the polymer reaction approach works, it is time-consuming and troublesome in procedure. We thus tried to polymerize the acetylenic monomers containing acidic protons directly. We first endeavored to polymerize **1** and found with delight that it could be directly transformed to its polymer (P**1**) by the polymerization reactions catalyzed by the organorhodium catalysts of [Rh(cod)Cl]$_2$, [Rh(nbd)Cl]$_2$, and Rh$^+$(nbd)[C$_6$H$_5$B$^-$(C$_6$H$_5$)$_3$], where cod is 1,5-cyclooctadiene and nbd is 2,5-norbornadiene (Scheme 3). Encouraged by the exciting result, we proceeded to polymerize other functional acetylene monomers containing active hydrogen atoms, electron-donating oxy and amino groups, and electron-withdrawing carbonyl and nitro groups (**2**−**5**). Although we have previously succeeded in polymerizing acetylenic monomers bearing azo,[18] cyano,[2] and thiol[10] groups, the polymerization of nitroacetylene monomers such as **5** had been difficult. Delightfully, the polymerizations of monomers **2**−**5** proceeded smoothly, furnishing polymers (P**2**−P**5**) with high molecular weights and low polydispersity indexes (PDIs).

We have been interested in the fabrication of macroscopically processable hybrids of functionalized polyacetylenes and carbon nanotubes (CNTs).[4,10] In our previous work, we employed pyrene- and ferrocene-containing monosubstituted polyacetylenes, poly(phenylacetylene) (PPA), and disubstituted polyacetylenes in functionalizing and solubilizing CNTs. It was found that the PPA skeleton could wrap onto the surfaces of CNTs through π−π interactions. This suggests that many PPA derivatives can be used as dispersants for CNTs. We have prepared PPA−CNT nanohybrids that are soluble in common organic solvents. We hope to replace the organic solvents by water because water is environment friendly and water-soluble CNTs may find an array of high-tech applications.[19−23] In this work, using P**1**$^-$ and P**4**$^+$ and multiwalled carbon nanotubes (MWNTs), we succeeded in preparing water-miscible nanohybrids of P**1**$^-$/MWNT and P**4**$^+$/MWNT through a noncovalent functionalization approach. In this article, we demonstrate that the nanohybrids can be used as versatile platforms for facile preparation of multicomponent nanocomposites such as Ag and ZnO nanoparticle-decorated MWNT.

Results and Discussion

Monomers **1** and **3** were prepared according to our previously published experimental procedures,[10,24] whereas monomer **4** is commercially available and was purchased from Aldrich. Monomers **2** and **5** were prepared following the synthetic routes shown in Scheme 4. The esterification reaction of **1** with butane-1,4-diol (**6**) mediated by *N*,*N*′-dicyclohexylcarbodiimide (DCC), 4-dimethylaminopyridine (DMAP), and *p*-toluenesulfonic acid monohydrate (TsOH) in dichloromethane (DCM) gives monomer **2** in 86% yield. The palladium-catalyzed cross-coupling reaction of 1-bromo-4-nitrobenzene (**7**) with (trimethylsilyl)acetylene (**8**) produces trimethyl[2-(4-nitrophenyl)ethynyl]silane (**9**) in 90% yield, whose base-catalyzed desilylation affords the desired monomer **5** in 72% yield. All monomers, including the commercial product (**4**), were fully characterized by spectroscopic methods, from which satisfactory analysis data were obtained. (See the Experimental Section for details.) Although [Rh(cod)Cl]$_2$ and [Rh(nbd)Cl]$_2$ are commercially available, all organorhodium complexes used in this study were prepared in our laboratories using the literature methods.[25]

As mentioned above, the traditional metathesis catalysts of early transition-metal chlorides NbCl$_5$, TaCl$_5$, MoCl$_5$, and WCl$_6$ are usually effective for the polymerizations of only acetylenic monomers with no or low polarities. The metal halides are ineffective in polymerizing highly polar acetylenic monomers because of their incompatibility with the polar functional groups.[1] To polymerize monomers **1** and **2**, we tried different catalyst systems. Although organorhodium complexes are known to be tolerant of polarity and functionality, they were still deemed hopeless in initiating the polymerizations of acetylenic monomers with carboxy groups.[1,16] Masuda and Werner's groups have even found that acetic acid is an effective terminator for the Rh-catalyzed polymerizations.[26,27] Because of this, carboxy-containing polyacetylenes are normally prepared through indirect routes.[16,17] It is thus a challenge and also of fundamental importance to explore carboxy-tolerant catalyst systems. With the hope of finding such catalysts, we focused our attention on the organorhodium complexes.

We first attempted to use [Rh(cod)Cl]$_2$ as a catalyst to polymerize the well-known carboxy-containing acetylene monomer **1** in THF. Fortunately and excitingly, the polymerization of **1** could be directly initiated by the [Rh(cod)Cl]$_2$ catalyst. A yellow polymer (P**1**) with a weight-average molecular weight (M_w) of 322 800 and a PDI of 1.25 was obtained in 44.5% yield (Table 1, no. 1). During the polymerization process, insoluble product was formed, indicating that the solubility of the resultant polymer in THF is not very good. We tested the solubility of P**1** in other solvents and found that it could hardly be dissolved in DCM, chloroform, and toluene. The insolubility of P**1** in these solvents may be caused by the strong intra- and intermolecular hydrogen-bonding interactions between the carboxy groups in the pendants of the polymer chains. However, P**1** is completely soluble in methanol, DMF, and DMSO. The solvent−carboxy interactions may have disrupted the chain interactions and hence rendered the polymer dispersible in the solvents at the molecular level.

We noticed that TEA was an effective cocatalyst in the Rh-catalyzed polymerization reactions, which often greatly accelerated the polymerization rate and gave polymers with higher

Scheme 4

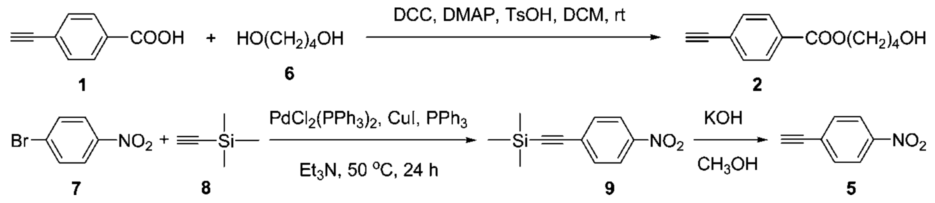

Table 1. Polymerizations of Monomers 1−5 Catalyzed by [Rh(diene)Cl]$_2$[a]

no.	catalyst	solvent	yield (%)	M_w[b]	M_w/M_n[b]	color
			1			
1	[Rh(cod)Cl]$_2$	THF	44.5	322 800	1.25	yellow
2	[Rh(cod)Cl]$_2$	THF/TEA	70.0	434 700	1.03	yellow
3	[Rh(nbd)Cl]$_2$	THF/TEA	60.9	403 900	1.06	yellow
			2			
4	[Rh(cod)Cl]$_2$	THF/TEA	21.7	190 100	1.30	yellow
5	[Rh(nbd)Cl]$_2$	THF/TEA	6.5	192 900	1.45	yellow
			3			
6	[Rh(cod)Cl]$_2$	THF	28.4	488 500	1.07	gray
7	[Rh(cod)Cl]$_2$	THF/TEA	39.2	nd		gray
8	[Rh(nbd)Cl]$_2$	THF/TEA	23.4	nd		gray
			4			
9	[Rh(cod)Cl]$_2$	THF/TEA	18.8	143 600	1.09	black
10	[Rh(nbd)Cl]$_2$	THF/TEA	18.7	106 800	1.72	black
			5			
11	[Rh(cod)Cl]$_2$	THF/TEA	29.6	113 800	1.52	brown-yellow
12	[Rh(nbd)Cl]$_2$	THF/TEA	61.6	137 200	1.22	gray-yellow

[a] Carried out under nitrogen at room temperature for 24 h. $[M]_0 = 0.5$ M, [cat.] = 2.5 mM. Abbreviations: cod, 1,5-cyclooctadiene; nbd, 2,5-norbornadiene; THF, tetrahydrofuran; TEA, triethylamine; nd, not determined (molecular weight exceeding the detection limit of the gel permeation chromatograph (GPC) columns). [b] Estimated by GPC in *N*,*N*-dimethylformamide (DMF).

molecular weights in higher yields.[1,10] When TEA was introduced to the polymerization mixture of **1**, the yield and M_w of P**1** were improved, and its PDI was narrowed (Table 1, no. 2). We then tried to use [Rh(nbd)Cl]$_2$ to polymerize **1**. This catalyst also worked well: P**1** with an M_w of 403 900 and a PDI of 1.06 was obtained in 61% yield (Table 1, no. 3). Prompted by the exciting results of the direct polymerization of **1** using the [Rh(diene)Cl]$_2$ catalysts, we proceeded to use them to polymerize other highly polar acetylene monomers. We designed and synthesized monomer **2**, a derivative of **1** that contains a hydroxy group. The monomer could also be polymerized to high-molecular-weight polymers, although the polymer yields were relatively low (Table 1, nos. 4 and 5).

In monomers **1** and **2**, an electron-withdrawing carbonyl group is attached to the phenyl ring. What would happen if an electron-donating group was attached to the phenyl ring? We chose monomers **3** and **4**, which contain electron-donating oxy and amino groups, respectively, to carry out the polymerization reactions. In both cases, polymeric products could be obtained (Table 1, nos. 6−10.). These results confirm that the acetylenes containing carboxy, hydroxy, and amino groups can all be polymerized by the rhodium catalysts regardless of whether their functional groups are electron-withdrawing or -donating. This indicates that it is unnecessary to take the indirect protection−deprotection or polymer-reaction approach to prepare the acidic and alcoholic polyacetylenes.

Besides the active hydrogen-containing acetylenes, highly polar monomers such as nitro-containing acetylenes are also difficult to polymerize. We prepared monomer **5** and tried to polymerize it. The results were encouraging: polymers with high molecular weights were obtained in reasonable-to-good yields (Table 1, nos. 11 and 12). It is worth pointing out that all of the above polymers (P**1**−P**5**) are generally insoluble in nonpolar solvents because of the strong interactions between the polymer chains or the high polarity of the pendant groups. Even in THF, only P**2** has a reasonable solubility. The situation for P**5** is particularly severe: even its solubility in DMSO is low.

Table 2. Polymerizations of Monomers 1−5 Catalyzed by Zwitterionic Complex Rh$^+$(nbd)[C$_6$H$_5$B$^-$(C$_6$H$_5$)$_3$] in THF[a]

no.	yield (%)	M_w[b]	M_w/M_n[b]	color
		1		
1	36.3	116 700	1.47	gray
		2		
2	31.6	166 300	1.98	yellow
		4		
3	50.0	43 700	2.23	black-green
		5		
4	64.5	nd		yellow

[a] Carried out under nitrogen at room temperature for 24 h. $[M]_0 = 0.5$ M, [cat.] = 2.5 mM. [b] Determined by GPC in DMF; nd, not determined because the sample is insoluble in DMF.

We have learned from our own experience as well as from reference papers that the zwitterionic complex of Rh$^+$(nbd)[C$_6$H$_5$B$^-$(C$_6$H$_5$)$_3$] is a good catalyst for polymerizing monosubstituted acetylenes.[4,28] Compared with [Rh(diene)Cl]$_2$ catalysts, it does not need cocatalyst and generally yields polymers with moderate molecular weights. This is nicely suited to our system because a moderate molecular weight is helpful in reducing chain interactions and hence endowing the polymers with higher solubility. Polymerizations of different monomers were carried out in THF at room temperature using the zwitterionic complex as catalyst. The results are shown in Table 2. Except for P**5**, all other polymers have lower molecular weights and show better solubilities. The effects are more evident in the cases of P**1** and P**4**: when the zwitterionic catalyst is used, the resulting polymers can be completely dissolved in even THF, whereas their counterparts obtained from the [Rh(diene)Cl]$_2$ catalyst are partially soluble or insoluble in THF.

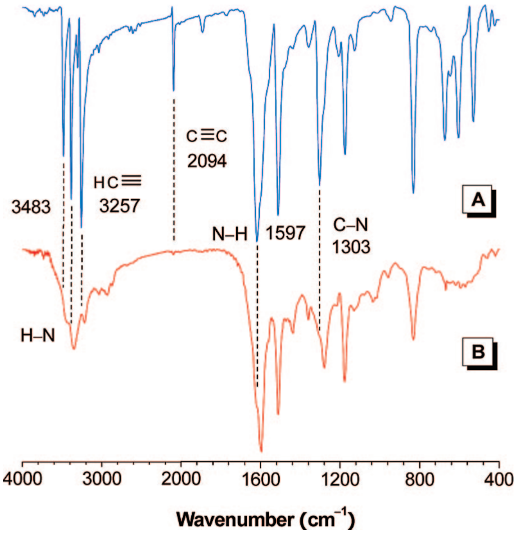

Figure 1. IR spectra of (A) monomer **4** and (B) its polymer P**4**.

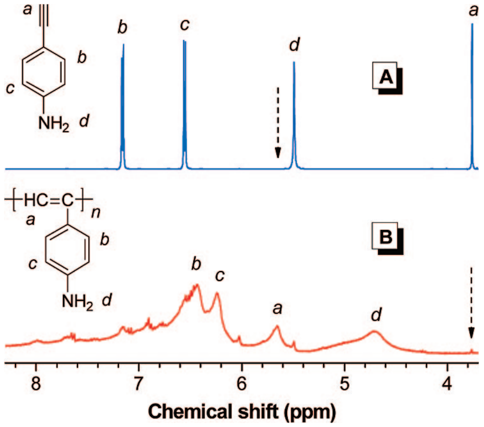

Figure 2. ^{1}H NMR spectra of (A) monomer **4** and (B) its polymer P**4** (sample taken from Table 2, no. 3) in DMSO-d_6.

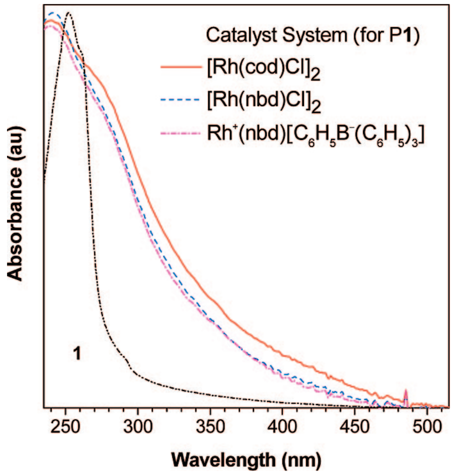

Figure 3. UV–vis spectra of monomer **1** and its polymer P**1** measured in methanol at room temperature. Concentration = 1.8 × 10^{-5} M.

Scheme 5

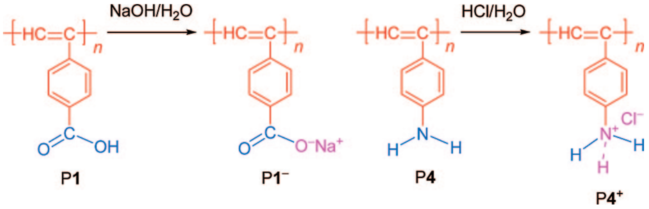

Structural Characterization. The polymers were characterized spectroscopically. An example of the IR spectrum of P**4** is shown in Figure 1B. Its monomer **4** exhibits absorption bands at 3257 and 2094 cm^{-1} because of the stretching vibrations of ≡CH and C≡C, respectively. These bands completely disappear in the spectrum of P**4**, indicating that the triple bond of **4** has been fully consumed by the polymerization reaction. The bands at 3483, 3385, and 1597 cm^{-1} due to N–H stretching and bending vibrations and the band at 1303 cm^{-1} due to C–N stretching vibration all remain almost unchanged in the spectrum of P**4**, suggesting that the amino functional group has remained intact during the polymerization process.

NMR spectroscopy provides valuable information about the macromolecular structures. As can be seen from the ^{1}H NMR spectrum of P**4**, there is no resonance peak at δ 3.76, which is associated with the acetylene proton (Figure 2B). A new peak due to the resonance of olefinic protons that is absent in the spectrum of its monomer appears at δ 5.65 (Figure 2A). The spectral data testify that the polymerization reaction has transformed the acetylenic triple bond of **4** to the olefinic double bond of P**4**. After polymerization, because of its electron-rich property, the conjugated polyene main chain of P**4** exerts a shielding effect on the phenyl protons, thus upfield-shifting their resonance peaks. Whereas the resonance peaks of the phenyl protons in **4** occur at δ 7.01 and 7.10, these peaks are shifted to δ 6.43 and 6.24 in the spectrum of P**4**. The resonance peak of the amino protons upfield shifts from δ 5.49 to 4.71 upon polymerization, which should be mainly caused by the strong association between the amino groups in the polymer. Like the IR spectra, the ^{1}H NMR spectra confirm that the acetylenic triple bond of **4** has been successfully transformed to the olefinic double bond of P**4** by the polymerization reaction.

Figure 3 shows the UV–vis absorption spectra of **1** and P**1**. Whereas **1** absorbs weakly at wavelengths beyond 300 nm, P**1** shows stronger absorption in the long wavelength region because of its conjugated polyene backbone. The absorption spectra for the polymer samples prepared by different catalysts are similar, indicating that the catalysts have exerted little effect on the conformational structure, effective conjugation, and electronic transitions of P**1**.

Fabrication of Water-Soluble Polyacetylene/Multiwalled Carbon Nanotube Hybrids. The polymers are composed of hydrophobic PPA skeleton and hydrophilic pendants. Because of this structural feature, the polymers are not soluble in common organic solvents as well as aqueous media. Ionizations of polyacid P**1** and polyamine P**4** by sodium hydroxide and hydrochloric acid furnish polyanion P**1**$^-$ and polycation P**4**$^+$, respectively (Scheme 5), which are soluble in water. The contrast between the good solubility of the polyelectrolytes in the aqueous media and the poor solubility of their parent forms of neutral polymers in the organic solvents testifies that there exist strong intra- and intermolecular interactions between the polymer chains of P**1** and P**4** that make them difficult to dissolve. The charges in the pendants of P**1**$^-$ and P**4**$^+$ not only reduce the chain interactions but also hamper chain aggregation or folding through electrostatic repulsion.

In our previous work, we found that substituted polyacetylenes, particularly PPA derivatives, readily wrapped onto the surfaces of CNTs through π–π interactions between the polymer chains and the CNT walls.[4,10] P**1**$^-$ and P**4**$^+$ are thus promising dispersants for CNTs because they are PPA derivatives. Indeed, by mixing the polyelectrolytes with MWNT in water, soluble P**1**$^-$/MWNT and P**4**$^+$/MWNT nanohybrids were obtained after removing the insoluble MWNT by filtering the

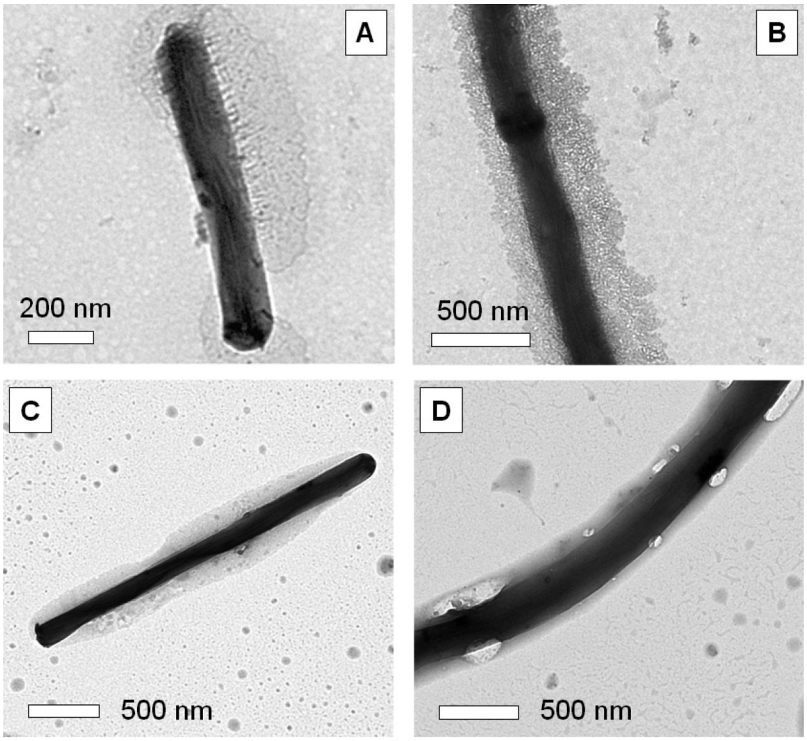

Figure 4. TEM images for (A,B) $P\mathbf{1}^-$/MWNT and (C,D) $P\mathbf{4}^+$/MWNT hybrids (samples taken from their aqueous solutions).

mixtures through cotton filters. The hybrids not only enjoy high solubility in water, an environmental friendly solvent, but also offer the promise of compounding with other materials. To study the microstructures of the hybrids, we took their transmission electron microscope (TEM) images. As can be seen from Figure 4, the MWNTs are clearly wrapped by polymer layers. This is particularly evident in the case of $P\mathbf{4}^+$/MWNT hybrid, in which a typical MWNT/polymer core/shell structure is observed. It is the polyelectrolyte layer that has made the MWNT soluble in the aqueous medium.

The polyelectrolytes $P\mathbf{1}^-$ and $P\mathbf{4}^+$ are thus qualified dispersants for MWNT dissolution in water. To evaluate their solvating powers quantitatively, we measured the solubilities of the nanohybrids in water by using eq 1

$$c = \frac{W_{\mathrm{MWNT}} - (W_{\mathrm{F}} - W_{\mathrm{F,0}})}{V_{\mathrm{S}}} \qquad (1)$$

where c is the concentration of MWNTs in a solvent (water), W_{MWNT} is the original weight of MWNT, W_{F} and $W_{\mathrm{F,0}}$ are the weights of the cotton filter after and before filtration, respectively, and V_{s} is the volume of solvent. Therefore, $(W_{\mathrm{F}} - W_{\mathrm{F,0}})$ and $W_{\mathrm{MWNT}} - (W_{\mathrm{F}} - W_{\mathrm{F,0}})$ are the weights of insoluble and soluble MWNTs that were retained by and passed through the filter, respectively. We also conducted the solubility tests on the PPA-functionalized MWNT in THF. For the purpose of comparison, all measurements were carried out under identical conditions.

The solubility data are summarized in Figure 5. The solvating powers of $P\mathbf{1}^-$ and $P\mathbf{4}^+$ to MWNT in water are 200 and 316 mg/L, respectively, and are much higher than that of PPA in THF (100 mg/L). The enhanced solvating powers of $P\mathbf{1}^-$ and $P\mathbf{4}^+$ are ascribed to the synergistic effects of the PPA skeleton and the mutually repulsive functional pendants.[29,30] Surfactants are known dispersants for CNTs.[31] $P\mathbf{1}^-$ and $P\mathbf{4}^+$ act in a way similar to that of surfactants in addition to their $\pi-\pi$ interactions with the MWNT. Interestingly, $P\mathbf{4}^+$ shows a higher solvating power than does $P\mathbf{1}^-$. Although the exact reason is not known, after comparing the chemical structures of the polyelectrolytes, we speculate that the more-crowded repulsive pendants may bring about higher solvating power. Another possible reason is the difference between the electron-donating and -withdrawing characteristics of their pendant groups because we have recently found that donor−acceptor interactions between electron-donating pendants and CNTs are helpful in dissolving CNTs.[30]

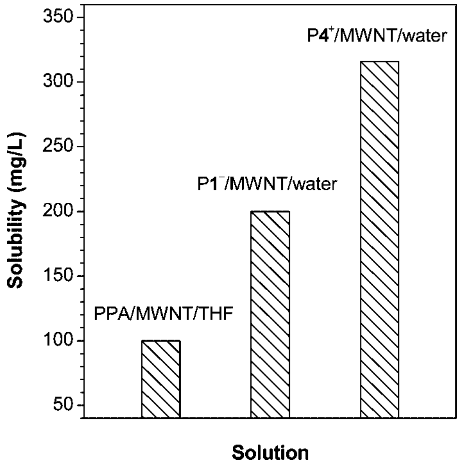

Figure 5. Solubilities of the MWNTs wrapped by PPA chains in THF and by $P\mathbf{1}^-$ and $P\mathbf{4}^+$ chains in water.

Preparation of Nanoparticle-Decorated Multiwalled Carbon Nanotube Hybrids. As water-soluble hybrid materials, the polyelectrolyte/MWNT composites are interesting in their own right because they may exhibit an array of unique properties. The hybrids may also be useful as versatile platforms for a variety of applications; for example, they may be employed in fabricating multilayer CNT-containing films through the layer-by-layer assembling process and in immobilizing biological molecules onto CNTs.[32] They may also be used to generate functional nanoparticle-decorated CNTs, which may find applications in catalysis, biology, nanotechnology, nanodevices, and so on.[20] We endeavored to explore these possibilities; we

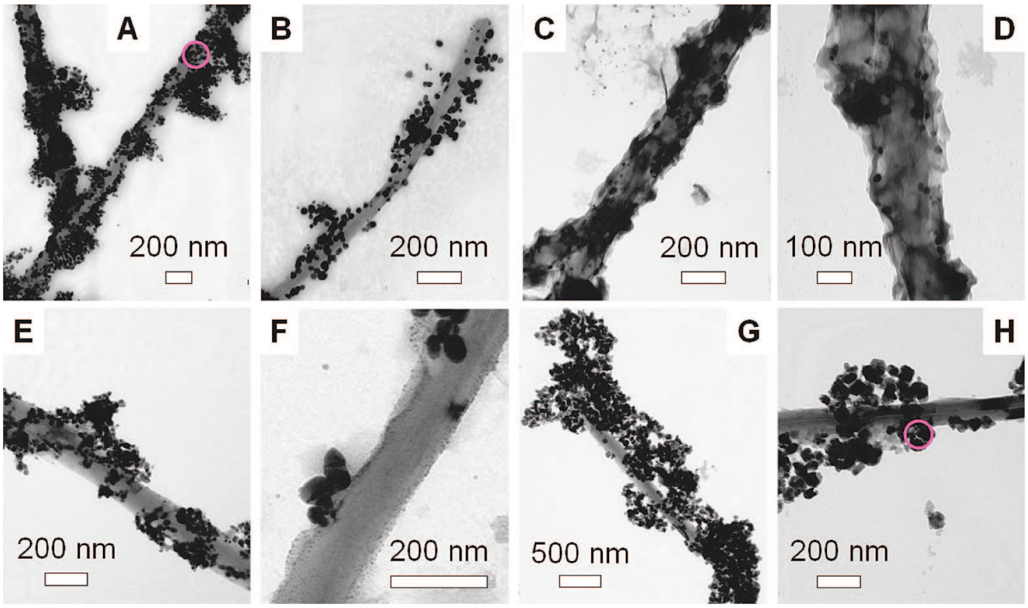

Figure 6. TEM images of the nanohybrids of (A,B) **P1**$^-$/MWNT/Ag (prepared using $NaBH_4$ as reductant), (C,D) **P1**$^-$/MWNT/Ag (using HCHO as reductant), (E,F) **P4**$^+$/MWNT/Ag, and (G,H) **P4**$^+$/MWNT/ZnO.

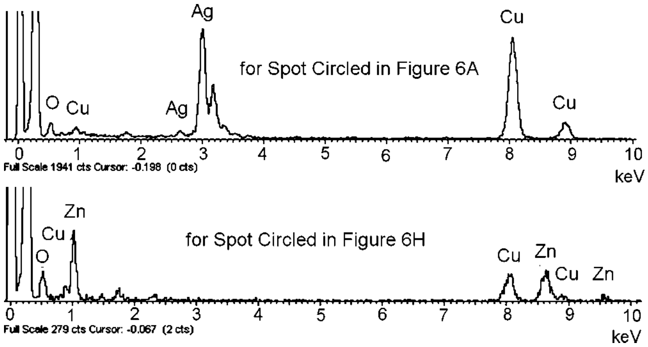

Figure 7. EDX spectra for the spots encircled in panels A and H in Figure 6.

herein report our effort in preparing Ag or ZnO nanoparticle-decorated MWNTs.

Because the **P1**$^-$/MWNT hybrids are negatively charged, positively charged metallic cations should be adsorbed onto their surfaces through electrostatic attractions. Metal nanoparticles can thus be deposited on the MWNT surfaces by the reduction of the metallic cations with appropriate reducing agents. The **P4**$^+$/MWNT hybrids carry positively charged ammonium pendant groups. Various ammonium salts, for example, tetraalkylammonium halides, have been used as stabilizers or passivators in the fabrication of metal cluster,[33,34] suggesting that prefabricated nanoparticles can be directly attached to the MWNT surfaces of the **P4**$^+$/MWNT hybrids. We tested these ideas using the procedures sketched in Scheme 6.

TEM observation is a direct and effective way to check if the idea works. As can be seen from the TEM images shown in Figure 6, multicomponent nanohybrids are indeed formed. In the **P1**$^-$/MWNT system, by absorption via electrostatic interactions and in situ reduction with $NaBH_4$, the silver cations (Ag^+) are transformed to silver (Ag) nanoparticles with diameters of ∼10−50 nm that are densely bound to the MWNT walls (Figure 6, panels A and B). The spot circled in Figure 6A was scrutinized by energy-dispersive X-ray (EDX) spectroscopy and was confirmed to be silver nanoparticles (Figure 7, upper panel). When formaldehyde (HCHO) was used as reductant, the morphologies of the resultant hybrids were quite different from those obtained from the $NaBH_4$ counterpart. Thin silver coatings on the MWNT surfaces were predominantly formed, with silver nanoparticles embedded in the coating matrixes (Figure 6, panels C and D). The formation of these unique morphologies is understandable. The reduction of Ag^+ by HCHO under mild conditions is a classic mirror reaction; in the presence of MWNT, the silver metal naturally forms overcoats on the tube surfaces.

In the **P4**$^+$/MWNT system, the preformed Ag and ZnO nanoparticles are adsorbed on the MWNT surfaces (Figure 6, panels E−H), which is suggestive of strong interactions between **P4**$^+$ and the nanoparticles. As can be seen from Figure 6F, the silver nanoparticles are ∼50 nm in size; as demonstrated by Figure 6G, the MWNT is surrounded by thousands of ZnO nanoparticles. Intriguingly, many of the particles are not in direct contact with the MWNT wall, implying that the nanoparticles are threaded through **P4**$^+$ chains. Zn and O elements are found in the EDX spectrum of the spot circled in Figure 6H, confirming the existence of ZnO nanoparticles in the nanocomposite (Figure 7, lower panel). This prefabrication postadsorption strategy offers a versatile means for the integration of various kinds of nanoparticles of different size and shape with MWNT and for the generation of nanohybrid materials with tunable compositions, morphologies, and properties.

As mentioned above, ammonium salts have been widely used as stabilizers in the fabrication of metallic cluster.[33,34] The precise chemical and physical basis of the stabilizing interactions, however, has not been satisfactorily elucidated. Although we are not clear about the exact mechanisms for the composition of the **P4**$^+$/MWNT hybrids with the preformed nanoparticles, the following processes may be involved. The silver and zinc oxide nanoparticles may be attracted to **P4**$^+$ chains, with the chloride and oxide anions of the polyelectrolytes and nanoparticles serving as adhesive bridges, which may be depicted as $PPA{-}N^+H_3{\cdot}Cl^-Ag^+$ and $PPA{-}N^+H_3{\cdot}O^-Zn^+$, respectively. Partial acid dissociation or desalt of **P4**$^+$ in the aqueous medium may generate chain segments with amino groups, which coordinate with the silver nanoparticles to afford the nanocomposites ($PPA{-}NH_2{\cdot}Ag$).

The absorption spectra of the nanohybrids are shown in Figure 8. The spectrum of **P1**$^-$/MWNT is similar to that of **P1** but is deviated from the baseline because of the existence of MWNT. After decoration by the Ag nanoparticles, the resultant **P1**$^-$/

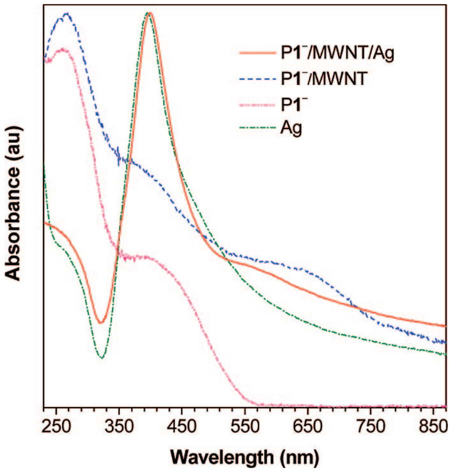

Figure 8. Absorption spectra of silver nanoparticles (Ag), polyelectrolyte **P1**$^-$, and its nanohybrids with MWNT (**P1**$^-$/MWNT) and silver nanoparticles (**P1**$^-$/MWNT/Ag, prepared using $NaBH_4$ as reductant) in water at room temperature.

MWNT/Ag nanocomposite shows a strong peak at 399 nm. This peak is due to the surface plasma excitation of the Ag particles,[35] as confirmed by the comparison with the spectrum of the pure Ag particles. These spectral data further verify the successful synthesis of the Ag-decorated MWNT nanocomposite.

Concluding Remarks

In this work, we have realized direct polymerizations of the phenylacetylene derivatives containing active hydrogen atoms (**1**−**4**) and a highly polar nitro group (**5**) by using rhodium complexes $[Rh(cod)Cl]_2$, $[Rh(nbd)Cl]_2$, and $Rh^+(nbd)[C_6H_5B^-(C_6H_5)_3]$ as catalysts. Whereas the electron-donating and -withdrawing nature of the functional group has exerted little effect on the polymerizability of the monomers, the catalysts affected the polymerization reactions, with the zwitterionic system yielding polymers with moderate molecular weights. The polymers exhibited rare molecular-weight-dependent solubility. Thus, the high-molecular-weight polymers prepared from the $[Rh(diene)Cl]_2$ catalysts are soluble in only the highly polar solvents (e.g., DMF and DMSO) because of the high polarity of the pendant groups and the strong interactions between the polymer chains. The polymers with moderate molecular weights prepared from the $Rh^+(nbd)[C_6H_5B^-(C_6H_5)_3]$ catalyst are more soluble and can be dissolved in such common solvent as THF.

Our achievement in polymerizing **1**−**4** by the organorhodium catalysts overturns the conventional conception that acetylenic monomers containing active protons, such as carboxy, hydroxy, and amino groups, could not be directly polymerized. Our success in the direct polymerization of the highly polar monomers paves the way for further developments in the design and syntheses of new functionalized polyacetylenes, particularly those with amino acid, sugar, and nucleoside pendants.

Polymers **P1** and **P4** can be facilely ionized to afford polyelectrolytes that are readily soluble in water. The ionization products **P1**$^-$ and **P4**$^+$ were used to prepare water-soluble **P1**$^-$/MWNT and **P4**$^+$/MWNT hybrids. The hybrids are miscible with aqueous media and may find applications as versatile platforms for the fabrication of functional hybrid materials such as multilayer CNT assembly films, CNT−protein bioconjugates, and nanoparticle-decorated CNT composites. As a demonstration of the facile realization of these attractive possibilities, we succeeded in the preparation of **P1**$^-$/MWNT/Ag, **P4**$^+$/MWNT/Ag, and **P4**$^+$/MWNT/ZnO multicomponent composites through direct deposition and prefabrication and postattachment approaches.

Experimental Section

Materials. THF was distilled under normal pressure from sodium benzophenone ketyl under argon immediately prior to use. TEA was distilled and dried over potassium hydroxide. Other solvents such as methanol, ethanol, and ethyl ether are of high purity and were used without further purification. 4-Ethynylbenzoic acid (**1**) and 6-(4-ethynylphenoxy)hexanoic acid (**3**) were prepared according to our previously published synthetic procedures.[10b,24] (Trimethylsilyl)acetylene (Acros), 4-ethynylaniline (**4**), dichlorobis(triphenylphosphine)palladium(II) (both from Aldrich), 1-bromo-4-nitrobenzene (Jiangsu Yancheng), DCC, DMAP, TsOH, butane-1,4-diol, copper(I) iodide, triphenylphosphine, sodium borohydride, silver nitrate, formaldehyde solution (all from SCRC) were used as received. ZnO nanoparticles were prepared in our laboratories by a solvothermal process. $[Rh(cod)Cl]_2$, $[Rh(nbd)Cl]_2$, and $Rh^+(nbd)[C_6H_5B^-(C_6H_5)_3]$ were prepared following literature methods.[25]

Instrumentations. ^1H and ^{13}C NMR spectra were measured on a Bruker ARX 500 spectrometer using $CDCl_3$ or DMSO-d_6 as solvent and tetramethylsilane (TMS, δ 0) as internal standard. IR spectra were recorded on a Bruker Vector 22 spectrometer. UV−vis absorption spectra were taken on a Varian Cary 100 Bio spectrophotometer. The thermal stability of the polymers was evaluated on a Perkin-Elmer Pyris thermogravimetric analyzer TGA 6. M_w, M_n, and M_w/M_n values of the polymers were estimated in DMF by a Waters 150 C GPC system. The measurement was carried out at an eluent flowing rate of 1 mL/min at 30 °C. MALDI-TOF spectra of the monomers were recorded on a GCT premier CAB048 mass spectrometer operating in a chemical ionization (CI) mode with methane as the carrier gas. Melting points were measured by the MELT-TEMP II melting point determination apparatus. TEM images were obtained on a JEOL/JEM-200 CX microscope coupled to an EDX analyzer.

Monomer Preparation. Monomers **2** and **5** were prepared according to the synthesis routes shown in Scheme 3. Detailed experimental procedures are given below.

*4-Hydroxybutyl-4-ethynylbenzoate (**2**).* In a 250 mL two-necked round-bottomed flask were added 1.46 g (10 mmol) of **1**, 4.13 g (20 mmol) of DCC, 244 mg (2 mmol) of DMAP, and 380 mg (2 mmol) of TsOH. The flask was evacuated under vacuum and flushed with nitrogen three times. Then, 2.7 g (30 mmol) of **6** in 100 mL of DCM was injected into the flask. The resultant mixture was stirred at room temperature for 24 h. After the formed urea salts were filtered out, the filtrate was concentrated by a rotary evaporator. The crude product was purified by a silica gel column using a mixture of chloroform and acetone (10:1 by volume) as eluent. A light-yellow liquid was obtained in 86.0% yield. IR (KBr) ν (cm^{-1}): 3418 (s, −OH), 3291 (s, HC≡), 2104 (s, C≡C), 1716 (s, C=O). ^1H NMR (500 MHz, DMSO-d_6) δ (TMS): 7.96 (d, 2H, aromatic protons ortho to −COO), 7.63 (d, 2H, aromatic protons meta to −COO), 4.51 (1H, −OH), 4.50 (s, 1H, HC≡), 4.29 (t, 2H, $-COOCH_2$), 3.47 (m, 2H, $-CH_2OH$), 1.75 (m, 2H, $-COOCH_2CH_2$), 1.56 (m, 2H, $-CH_2CH_2OH$). ^{13}C NMR (75 MHz, DMSO-d_6) δ (TMS): 165.4 (C=O), 132.4 (aromatic carbon meta to C=O), 130.3, 129.6 (aromatic carbons linked and ortho to C=O), 126.8 (aromatic carbon linked to ≡C), 84.1 (≡C), 83.0 (HC≡), 65.3 ($-COOCH_2$), 60.7, ($-CH_2OH$), 29.3 ($-CH_2CH_2OH$), 25.4 ($-COOCH_2CH_2$). HRMS (MALDI-TOF): Anal. Calcd for $C_{13}H_{14}O_3$: 218.0943. Found: 219.1018 [(M + H)$^+$].

*Trimethyl[2-(4-nitrophenyl)ethynyl]silane (**9**).* To a 250 mL two-necked round-bottomed flask were added 104.2 mg (0.2 mmol) of $PdCl_2(PPh_3)_2$, 76.2 mg (0.4 mmol) of CuI, 52.5 mg (0.2 mmol) of PPh_3, and 100 mL of a TEA solution of 1-bromo-4-nitrobenzene (**7**; 7, 2.02 g, 10 mmol) under an atmosphere of nitrogen. After the catalysts were completely dissolved, 1.6 mL (11 mmol) of (trimethylsilyl)acetylene (**8**) was injected into the flask, and the mixture was stirred at 50 °C for 24 h. The formed solid was removed by filtration and washed with diethyl ether. The filtrate was then concentrated by a rotary evaporator. The crude product was purified on a silica gel column with hexane as eluent. A light-yellow solid

Scheme 6

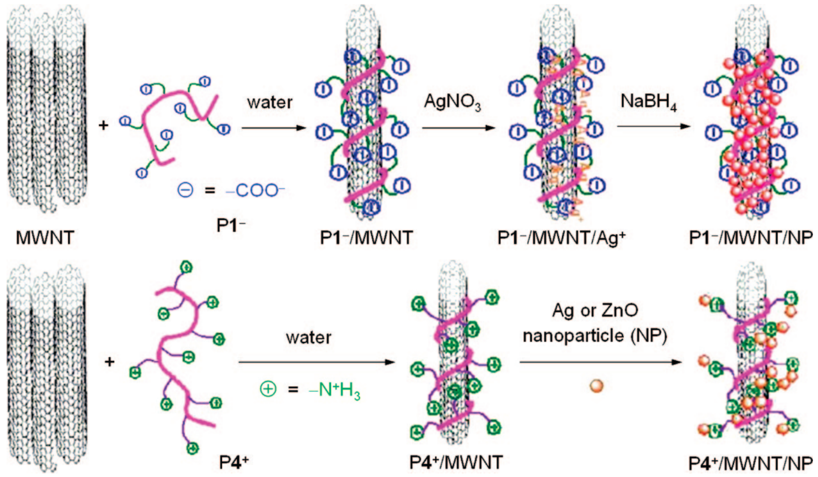

of **9** was obtained in 90.3% yield (1.98 g). IR (KBr) ν (cm^{-1}): 2159 (m, C≡C), 1519 (vs, $-$NO$_2$), 1347 (vs, $-$NO$_2$). ^{1}H NMR (500 MHz, CDCl$_3$) δ (TMS): 8.16 (d, aromatic protons ortho to $-$NO$_2$), 7.59 (d, aromatic protons meta to $-$NO$_2$), 0.28 (s, $-$Si(CH$_3$)$_3$). ^{13}C NMR (75 MHz, CDCl$_3$) δ (TMS): 147.13 (aromatic carbon linked to $-$NO$_2$), 132.7 (aromatic carbons meta to $-$NO$_2$), 130.0 (aromatic carbon linked to ≡C), 123.5 (aromatic carbons ortho to $-$NO$_2$), 102.7 (≡C$-$Ar) 100.6 (≡C$-$Si), $-$0.32 ($-$Si(CH$_3$)$_3$). HRMS (MALDI-TOF): Anal. Calcd for $C_{13}H_{13}NO_2Si$: 219.0716. Found: 219.0797 [(M)$^+$]. mp 96$-$97 °C.

*1-Ethynyl-4-nitrobenzene (**5**).* To a 100 mL round-bottomed flask equipped with a reflux condenser were added 1.0 g (5 mmol) of **9**, 50 mL of methanol, and 1.1 g (20 mmol) of KOH. The contents were refluxed for 5 h. The mixture was concentrated by a rotary evaporator, washed by excess dilute hydrochloric acid, and extracted with DCM three times. The DCM solution was then washed by saturated NaHCO$_3$ and NaCl solutions. The mixture was dried over 5 g of magnesium sulfate. The crude product was condensed and purified on a silica gel column using hexane as eluent. A pale-yellow solid of **5** was obtained in 72.0% yield (0.53 g). IR (KBr) ν (cm^{-1}): 3252 (s, HC≡), 2102 (m, C≡C), 1513 (vs, $-$NO$_2$), 1344 (vs, $-$NO$_2$). ^{1}H NMR (500 MHz, CDCl$_3$) δ (TMS): 8.19 (d, aromatic protons ortho to $-$NO$_2$), 7.63 (d, aromatic protons meta to $-$NO$_2$), 3.36 (s, HC≡). ^{13}C NMR (75 MHz, CDCl$_3$) δ (TMS): 147.5 (aromatic carbon linked to $-$NO$_2$), 132.9 (aromatic carbon meta to $-$NO$_2$), 128.8, (aromatic carbon linked to ≡C), 123.5 (aromatic carbon ortho to $-$NO$_2$), 82.3 (≡C), 81.5 (HC≡). HRMS (MALDI-TOF): Anal. Calcd for $C_8H_5NO_2$: 147.0320. Found: 148.0393 [(M + H)$^+$]. mp 150$-$151 °C.

Monomers **1** and **3** were prepared according to our published procedures,[10b,24] whereas monomer **4** was purchased from Aldrich. Characterization data for the monomers are given below. 4-Ethynylbenzoic acid (**1**): IR (KBr) ν (cm^{-1}): 3272 (s, HC≡), 1688 (s, C=O). ^{1}H NMR (500 MHz, DMSO-d_6): 7.91 (d, 2H, aromatic protons ortho to C=O), 7.60 (d, 2H, aromatic protons meta to C=O), 4.35 (s, 1H, HC≡). ^{13}C NMR (75 MHz, DMSO-d_6): 166.7 (C=O), 132.0 (aromatic carbons meta to C=O), 131.0 (aromatic carbon linked to C=O), 129.5 (aromatic carbons ortho to C=O), 126.0 (aromatic carbon linked to $-$C≡CH), 83.6 (C≡), 82.8 (≡CH). HRMS (MALDI-TOF): Anal. Calcd for $C_9H_6O_2$: 146.0368. Found: 147.0447 [(M + H)$^+$]. mp 224 °C dec. 6-(4-Ethynylphenoxy)hexanoic acid (**3**): IR (KBr) ν (cm^{-1}): 3297 (s, HC≡C), 2106 (m, C≡C), 1706 (s, C=O). ^{1}H NMR (500 MHz, DMSO-d_6): 7.34 (d, 2H, aromatic protons meta to $-$O$-$), 6.88 (d, 2H, aromatic protons ortho to $-$O$-$), 3.97 (s, 1H, HC≡), 3.93 (t, 2H, $-$OCH$_2$), 2.18 (t, 2H, $-$CH$_2$COO), 1.66 (m, 2H, $-$OCH$_2$C*H*$_2$), 1.48 (m, 2H, $-$C*H*$_2$CH$_2$COOH), 1.35 (m, 2H, CH$_2$). ^{13}C NMR (75 MHz, DMSO-d_6): 175.1 (C=O), 159.7 (aromatic carbon linked to $-$O$-$), 133.9 (aromatic carbon meta to $-$O$-$), 115.4 (aromatic carbon ortho to $-$O$-$), 114.2 (aromatic carbon linked to $-$C≡CH), 84.3 (C≡), 79.8 (≡CH), 68.2 ($-$OCH$_2$), 34.3 ($-$*C*H$_2$COO), 29.0 ($-$OCH$_2$*C*H$_2$), 25.8 ($-$*C*H$_2$CH$_2$COO), 24.9 (CH$_2$). HRMS (MALDI-TOF): Anal. Calcd for $C_{14}H_{16}O_3$: 232.1099. Found: 233.1174 [(M + H)$^+$]. mp 80$-$82 °C. 4-Ethynylaniline (**4**): IR (KBr) ν (cm^{-1}): 3483 (s, N$-$H), 3257 (s, HC≡), 2094 (m, C≡C), 1597 (s, N$-$H), 1303 (C$-$N). ^{1}H NMR (500 MHz, DMSO-d_6): 7.15 (d, 2H, aromatic protons meta to $-$NH$_2$), 6.55 (d, 2H, aromatic protons ortho to $-$NH$_2$), 5.49 (s, 2H, $-$NH$_2$), 3.76 (s, 1H, HC≡). ^{13}C NMR (75 MHz, DMSO-d_6): 149.9 (aromatic carbon linked to $-$NH$_2$), 133.3 (aromatic carbon meta to $-$NH$_2$), 114.0 (aromatic carbon ortho to $-$NH$_2$), 108.3 (aromatic carbon linked to $-$C≡CH), 85.6 (≡C), 77.6 (≡CH). HRMS (*m*/*z*): Anal. Calcd for C_8H_7N: 117.0579. Found: 118.0651 [(M + H)$^+$]. mp 102$-$103 °C.

Polymer Synthesis. All polymerization reactions and manipulations were carried out under nitrogen using Schlenk techniques in a vacuum-line system except for the purification of the resultant polymers, which was done in an open atmosphere. The synthesis route to the polymers is shown in Scheme 2. Typical experimental procedures for the polymerization of monomer **4** in THF using Rh$^+$(nbd)[C$_6$H$_5$B$^-$(C$_6$H$_5$)$_3$] as catalyst are given below as an example.

To a 20 mL Schlenk tube with a sidearm was added 117 mg (1 mmol) of **4**. The tube was evacuated under vacuum and then flushed with nitrogen three times through the sidearm. Then, 1 mL of THF was injected. The catalyst solution was prepared in another tube by dissolving 2.3 mg of Rh$^+$(nbd)[C$_6$H$_5$B$^-$(C$_6$H$_5$)$_3$] in 1 mL of THF. After aging for 15 min, the solution was transferred to the monomer solution using a hypodermic syringe. The reaction mixture was stirred at room temperature under nitrogen for 24 h. The resulting mixture was diluted with 5 mL of THF and added dropwise through a cotton filter to 500 mL of hexane under stirring. The precipitate was allowed to stand for 24 h and was then filtered with a Gooch crucible. The polymer was washed with hexane five times and dried in a vacuum oven at 40 °C to a constant weight.

*Characterization Data for P**4** (Table 2, no. 3).* Dark-green solid, yield: 50.0%. M_w: 43 700; M_w/M_n: 2.23. IR (KBr) ν (cm^{-1}): 1279 (s, C$-$N), 1598 (s, N$-$H), 3351 (s, N$-$H). ^{1}H NMR (500 MHz, DMSO-d_6) δ (TMS): 6.43 (2H, aromatic protons meta to $-$NH$_2$), 6.24 (2H, aromatic protons ortho to $-$NH$_2$), 5.65 (s, $-$HC=C), 4.71 (s, 2H, $-$NH$_2$).

*P**1** (Table 1, no. 1).* Yellow solid, yield: 44.5%. M_w: 322 800; M_w/M_n: 1.25. IR (KBr) ν (cm^{-1}): 1703 (s, C=O). ^{1}H NMR (500 MHz, DMSO-d_6) δ (TMS): 7.93, 7.60 (aromatic protons), 5.88 ($-$HC=C, a very small but discernible peak).

*P**2** (Table 1, no. 4).* Yellow solid, yield: 21.7%. M_w: 190 100; M_w/M_n: 1.30. IR (KBr) ν (cm^{-1}): 3431 (s, $-$OH), 1716 (s, C=O). ^{1}H NMR (500 MHz, DMSO-d_6) δ (TMS): 7.47 (aromatic protons ortho to $-$COO), 6.70 (aromatic protons meta to $-$COO), 5.77 (1H, $-$HC=C), 4.14 (2H, $-$COOCH$_2$), 3.39 (2H, $-$CH$_2$O), 1.69 (2H, $-$COOCH$_2$C*H*$_2$), 1.44 (2H, $-$C*H*$_2$CH$_2$OH).

*P**3** (Table 1, no. 7).* Grey solid, yield: 39.2%. IR (KBr) ν (cm^{-1}): 1708 (s, C=O). ^{1}H NMR (500 MHz, DMSO-d_6) δ (TMS): 11.94

($-$COOH), 7.50 (2H, aromatic protons meta to $-$O$-$), 6.95 (2H, aromatic protons ortho to $-$O$-$), 3.98 (2H, $-\mathrm{OCH_2}$), 2.21 (2H, $-\mathrm{CH_2COO}$), 1.69 (2H, $-\mathrm{OCH_2C}H_2$), 1.53 (2H, $-\mathrm{CH_2CH_2COO}$), 1.40 (2H, $-\mathrm{OCH_2C}H_2\mathrm{CH_2}$).

*P***5** *(Table 1, no. 12).* Grey-yellow solid, yield: 61.6%. M_w: 137 200; M_w/M_n: 1.22. IR (KBr) ν (cm^{-1}): 1518 (s, $-\mathrm{NO_2}$), 1344 (s, $-$NO2). The NMR data were not obtained because the solubility of the polymer in common organic solvents, such as chloroform, DCM and DMSO, is extremely low.

Preparation of Polyelectrolytes. Water-soluble polyelectrolytes P**1**$^-$ and P**4**$^+$ were prepared by ionizations of P**1** and P**4** using dilute sodium hydroxide and hydrochloric acid solutions, respectively. The preparation of P**1**$^-$ is described below as an example: 50 mg of P**1** was added to 10 mL of 0.5 M sodium hydroxide solution. After the polymer was completely dissolved, the mixture was added dropwise to 200 mL of ethanol under stirring. The precipitate was collected by filtration, washed with ethanol, and dried under vacuum at 40 °C to a constant weight.

Polyelectrolyte/Multiwalled Carbon Nanotube Hybridization. The procedures for the preparation of P**1**$^-$/MWNT hybrid are given below as an example. To a tube were added 4.0 mg of P**1**$^-$, 5.0 mg of MWNT, and 3 mL of water. After vigorous stirring for 1 h, the mixture was filtered through a cotton filter to remove the unwrapped, insoluble MWNT. The filter was dried under vacuum at 100 °C to a constant weight.

Fabrication of Silver Nanoparticles. To a 20 mL tube containing 4 mL of $\mathrm{AgNO_3}$ solution (2×10^{-3} M) was added excess $\mathrm{NaBH_4}$ solution (3×10^{-3} M) dropwise under vigorous stirring. The silver nanoparticles were formed instantaneously.

Nanoparticle/Polyelectrolyte/Multiwalled Carbon Nanotube Composition. After centrifugation under 10 000 rpm for 10 min, the precipitated P**1**$^-$/MWNT hybrid was collected. A small amount of the hybrid was redissolved in 2 mL of water, and 2 mL of $\mathrm{AgNO_3}$ (10^{-3} M) was then added slowly under vigorous stirring. After stirring for 10$-$15 min, two methods were adopted to reduce the silver ions. One method was the addition of excess $\mathrm{NaBH_4}$ solution (3×10^{-3} M) dropwise under vigorous stirring at room temperature. The other method was to use HCHO solution as a reductant at 80 °C for 4 h. The mixtures were then centrifuged at 10 000 rpm for 10 min again. The precipitate was collected and redispersed in water for testing.

For the P**4**$^+$/MWNT hybrid, after centrifugation and redispersing in water, a small amount of Ag or ZnO nanoparticles was directly added to the hybrids under vigorous stirring.

Acknowledgment. The work reported in this article was partially supported by the National Science Foundation of China (20634020 and 50573065), the Research Grants Council of Hong Kong (603008, 601608, and 602707), the Ministry of Science and Technology of China (2009CB623600), and the Nanoscience and Nanotechnology Program at HKUST. B.Z.T. acknowledges the support from the Cao Guangbiao Foundation of Zhejiang University.

Supporting Information Available: TGA thermograms of P**1**$-$P**5**. This material is available free of charge via the Internet at http://pubs.acs.org.

References and Notes

(1) (a) Lam, J. W. Y.; Tang, B. Z. *J. Polym. Sci., Part A: Poly. Chem.* **2003**, *41*, 2607. (b) Lam, J. W. Y.; Tang, B. Z. *Acc. Chem. Res.* **2005**, *38*, 745. (c) Masuda, T. *J. Polym. Sci., Part A: Poly. Chem.* **2007**, *45*, 165. (d) Yashima, E.; Maeda, K.; Furusho, Y. *Acc. Chem. Res.* **2008**, *41*, 1166. (e) Tang, B. Z. *Macromol. Chem. Phys.* **2008**, *209*, 1304. (f) Li, C.; Li, Y. *Macromol. Chem. Phys.* **2008**, *209*, 1541. (g) Rudick, J. G.; Percec, V. *Macromol. Chem. Phys.* **2008**, *209*, 1760. (h) Kwak, G.; Jin, S.-H.; Park, J.-W.; Gal, Y.-S. *Macromol. Chem. Phys.* **2008**, *209*, 1769.

(2) (a) Tang, B. Z.; Kong, X.; Wan, X.; Feng, X.-D.; Kwok, H. S. *Macromolecules* **1998**, *31*, 2419. (b) Kong, X.; Lam, J. W. Y.; Tang, B. Z. *Macromolecules* **1999**, *32*, 1722. (c) Lam, W. Y.; Dong, Y.; Cheuk, K. L.; Luo, J.; Kwok, H. S.; Tang, B. Z. *Macromolecules* **2002**, *35*, 1229. (d) Lam, W. Y.; Dong, Y.; Tang, B. Z. *Macromolecules* **2002**, *35*, 8288. (e) Kwak, G.; Minakuchi, M.; Sakaguchi, T.; Masuda, T.; Fujiki, M. *Chem. Mater.* **2007**, *19*, 3654.

(3) (a) Kang, E. T.; Ehrlich, P.; Bhatt, A.; Anderson, W. *Macromolecules* **1984**, *17*, 1020. (b) Tang, B. Z.; Chen, H.; Lam, W. Y.; Wang, M. *Chem. Mater.* **2000**, *12*, 213.

(4) (a) Buchmeiser, M. R.; Schuler, N.; Kaltenhauser, G.; Ongania, K.-H.; Lagoja, I.; Wurst, K.; Schottenberger, H. *Macromolecules* **1998**, *31*, 3175. (b) Yuan, W. Z.; Mao, Y.; Zhao, H.; Sun, J. Z.; Xu, H. P.; Jin, J. K.; Zheng, Q.; Tang, B. Z. *Macromolecules* **2008**, *41*, 701. (c) Yuan, W. Z.; Sun, J. Z.; Liu, J. Z.; Dong, Y.; Li, Z.; Xu, H. P.; Qin, A. J.; Häussler, M.; Jin, J. K.; Zheng, Q.; Tang, B. Z. *J. Phys. Chem. B* **2008**, *112*, 8896.

(5) Tabata, M.; Sadahiro, Y.; Nozaki, Y.; Inaba, Y.; Yokota, K. *Macromolecules* **1996**, *29*, 6673.

(6) (a) Sanda, F.; Araki, H.; Masuda, T. *Macromolecules* **2004**, *37*, 8510. (b) Morino, K.; Maeda, K.; Yashima, E. *Macromolecules* **2003**, *36*, 1480. (c) Lai, L. M.; Lam, J. W. Y.; Qin, A.; Dong, Y.; Tang, B. Z. *J. Phys. Chem. B* **2006**, *110*, 11128. (d) Li, B. S.; Kang, S. Z.; Cheuk, K. K. L.; Wan, L.; Ling, L.; Bai, C.; Tang, B. Z. *Langmuir* **2004**, *20*, 7598. (e) Cheuk, K. K. L.; Lam, J. W. Y.; Chen, J.; Lai, L. M.; Tang, B. Z. *Macromolecules* **2003**, *36*, 5947. (f) Okoshi, K.; Kajitani, T.; Nagai, K.; Yashima, E. *Macromolecules* **2008**, *41*, 258.

(7) Cheuk, K. K. L.; Lam, J. W. Y.; Li, B. S.; Xie, Y.; Tang, B. Z. *Macromolecules* **2007**, *40*, 2633.

(8) (a) Yuan, W. Z.; Qin, A.; Lam, J. W. Y.; Sun, J. Z.; Dong, Y.; Häussler, M.; Liu, J.; Xu, H. P.; Zheng, Q.; Tang, B. Z. *Macromolecules* **2007**, *40*, 3159. (b) Qu, J.; Katsumata, T.; Satoh, M.; Wada, J.; Igarashi, J.; Mizoguchi, K.; Masuda, T. *Chem.—Eur. J.* **2007**, *13*, 7965.

(9) (a) Kishimoto, Y.; Eckerle, P.; Miyatake, T.; Ikariya, T.; Noyori, R. *J. Am. Chem. Soc.* **1994**, *116*, 12131. (b) Kishimoto, Y.; Eckerle, P.; Miyatake, T.; Kainosho, M.; Ono, A.; Ikariya, T.; Noyori, R. *J. Am. Chem. Soc.* **1999**, *121*, 12035. (c) Saeed, I.; Shiotsuki, M.; Masuda, T. *Macromolecules* **2006**, *39*, 8977. (d) Tang, B. Z.; Poon, W. H.; Leung, S. M.; Leung, W. H.; Peng, H. *Macromolecules* **1997**, *30*, 2209.

(10) (a) Tang, B. Z.; Xu, H. *Macromolecules* **1999**, *32*, 2569. (b) Yuan, W.; Sun, J. Z.; Dong, Y.; Häussler, M.; Yang, F.; Xu, H. P.; Qin, A.; Lam, J. W. Y.; Zheng, Q.; Tang, B. Z. *Macromolecules* **2006**, *39*, 8011. (c) Yuan, W. Z.; Zhao, H.; Xu, H. P.; Sun, J. Z.; Lam, J. W. Y.; Mao, Y.; Jin, J. K.; Zhang, S.; Zheng, Q.; Tang, B. Z. *Acta Polym. Sin.* **2007**, *10*, 901. (d) Hua, J.; Li, Z.; Lam, J. W. Y.; Xu, H.; Sun, J.; Dong, Y.; Dong, Y.; Qin, A.; Yuan, W.; Chen, H.; Wang, M.; Tang, B. Z. *Macromolecules* **2005**, *38*, 8127. (e) Xu, H.; Sun, J.; Qin, A.; Hua, J.; Li, Z.; Dong, Y.; Xu, H.; Yuan, W.; Ma, Y.; Wang, M.; Tang, B. Z. *J. Phys. Chem. B* **2006**, *110*, 21701. (f) Xu, H.-P.; Xie, B.-Y.; Yuan, W.-Z.; Sun, J.-Z.; Yang, F.; Dong, Y.-Q.; Qin, A.; Zhang, S.; Wang, M.; Tang, B. Z. *Chem. Commun.* **2007**, (13), 1322. (g) Xu, H.; Jin, J. K.; Mao, Y.; Sun, J. Z.; Yang, F.; Yuan, W.; Dong, Y. Q.; Wang, M.; Tang, B. Z. *Macromolecules* **2008**, *41*, 3874.

(11) Tang, B. Z.; Xu, H.; Lam, J. W. Y.; Lee, P. P. S.; Xu, K.; Sun, Q.; Cheuk, K. K. L. *Chem. Mater.* **2000**, *12*, 1446.

(12) Teraguchi, M.; Masuda, T. *Macromolecules* **2002**, *35*, 1149.

(13) (a) Tang, B. Z.; Kotera, N. *Macromolecules* **1989**, *22*, 4388. (b) Xu, K.; Peng, H.; Lam, W. Y.; Dong, Y.; Sun, Q.; Salhi, F.; Tang, B. Z. *Macromolecules* **2000**, *33*, 6918.

(14) Hirao, K.; Ishii, Y.; Terao, T.; Kishimoto, Y.; Miyatake, T.; Ikariya, T.; Noyori, R. *Macromolecules* **1998**, *31*, 3405.

(15) Sanda, F.; Yukawa, Y.; Masuda, T. *Polymer* **2004**, *45*, 849.

(16) (a) Maeda, K.; Goto, H.; Yashima, E. *Macromolecules* **2001**, *34*, 1160. (b) Saito, M. A.; Maeda, K.; Onouchi, H.; Yashima, E. *Macromolecules* **2000**, *33*, 4616. Yashima's group prepared the poly"acid" P**1** indirectly by the polymerizations of the derivatives of **1,** including its esters and water-soluble salt, followed by hydrolysis and acidification of the poly"esters" and poly"salts", respectively.

(17) (a) Li, B. S.; Cheuk, K. K. L.; Ling, L.; Chen, J.; Xiao, X.; Bai, C.; Tang, B. Z. *Macromolecules* **2003**, *36*, 77. (b) Cheuk, K. K. L.; Lam, J. W. Y.; Lai, L. M.; Dong, Y.; Tang, B. Z. *Macromolecules* **2003**, *36*, 9752. (c) Li, B. S.; Chen, J.; Zhu, C. F.; Leung, K. K. L.; Wan, L.; Bai, C.; Tang, B. Z. *Langmuir* **2004**, *20*, 2515. (d) Lai, L. M.; Lam, J. W. Y.; Cheuk, K. K. L.; Sung, H. H. Y.; Williams, I. D.; Tang, B. Z. *J. Polym. Sci., Part A: Polym. Chem.* **2005**, *43*, 3701. (e) Cheuk, K. K. L.; Li, B. S.; Lam, J. W. Y.; Xie, Y.; Tang, B. Z. *Macromolecules* **2008**, *41*, 5997.

(18) Yin, S.; Xu, H.; Shi, W.; Gao, Y.; Song, Y.; Lam, J. W. Y.; Tang, B. Z. *Polymer* **2005**, *46*, 7670.

(19) (a) Sun, Y.-P.; Fu, K.; Lin, Y.; Huang, W. *Acc. Chem. Res.* **2002**, *35*, 1096. (b) Pagona, G.; Sandanayaka, A. S. D.; Araki, Y.; Fan, J.; Tagmatarchis, N.; Yudasaka, M.; Iijima, S.; Ito, O. *J. Phys. Chem. B* **2006**, *110*, 20729. (c) Liu, Z.; Sun, X.; Nakayama-Ratchford, N.; Dai, H. *ACS Nano* **2007**, *1*, 50. (d) Prato, M.; Kostarelos, K.; Bianco, A. *Acc. Chem. Res.* **2008**, *41*, 60.

(20) Georgakilas, V.; Gournis, D.; Tzitzios, V.; Pasquato, L.; Guldi, D. M.; Prato, M. *J. Mater. Chem.* **2007**, *17*, 2679, and references therein.

(21) Gao, C.; Li, W.; Morimoto, H.; Nagaoka, Y.; Maekawa, T. *J. Phys. Chem. B* **2006**, *110*, 7213.

(22) (a) Li, X.; Liu, Y.; Fu, L.; Cao, L.; Wei, D.; Wang, Y. *Adv. Funct. Mater.* **2006**, *16*, 2431. (b) Wildgoose, G. G.; Banks, C. E.; Compton, R. G. *Small* **2006**, *2*, 182. (c) Niyogi, S.; Hamon, M. A.; Hu, H.; Zhao, B.; Bhowmik, P.; Sen, R.; Itkis, M. E.; Haddon, R. C. *Acc. Chem. Res.* **2002**, *35*, 1105. (d) Planeix, J. M.; Coustel, N.; Coq, J.; Brotons, V.; Kumbhar, P. S.; Dutartre, R.; Geneste, P.; Bernier, P.; Ajayan, P. M. *J. Am. Chem. Soc.* **1994**, *116*, 7935.

(23) (a) Kim, H. S.; Lee, H.; Han, K. S.; Kim, J. H.; Song, M. S.; Park, M. S.; Lee, J. Y.; Kang, J. K. *J. Phys. Chem. B* **2005**, *109*, 8983. (b) Ang, L. M.; Hor, T. S. A.; Xu, G. Q.; Tung, C. H.; Zhao, S. P.; Wang, J. L. S. *Chem. Mater.* **1999**, *11*, 2115. (c) Raghuveer, M. S.; Agrawal, S.; Bishop, N.; Ramanath, G. *Chem. Mater.* **2006**, *18*, 1390. (d) Giordano, R.; Serp, P.; Kalck, P.; Kihn, Y.; Schreiber, J.; Marhic, C.; Duvail, J.-L. *Eur. J. Inorg. Chem.* **2003**, 610. (e) Han, L.; Wu, W.; Kirk, F. L.; Maye, J.; Luo, M. M.; Kariuki, N. N.; Lin, Y.; Wang, C.; Zhong, C. J. *Langmuir* **2004**, *20*, 6019. (f) Sainsbury, T.; Stolarczyk, J.; Fitzmaurice, D. *J. Phys. Chem. B* **2005**, *109*, 16310. (g) Sainsbury, T.; Fitzmaurice, D. *Chem. Mater.* **2004**, *16*, 2174. (h) Ou, Y. Y.; Huang, M. H. *J. Phys. Chem. B* **2006**, *110*, 2031. (i) Stoffelbach, F.; Aqil, A.; Jerome, C.; Jerome, R.; Detrembleur, C. *Chem. Commun.* **2005**, (36), 4532. (j) Robel, I.; Bunker, B. A.; Kamat, P. V. *Adv. Mater.* **2005**, *17*, 2458.

(24) Tang, B. Z.; Kong, X.; Wan, X.; Feng, X.-D. *Macromolecules* **1997**, *30*, 5620.

(25) (a) *Dictionary of Organometallic Compounds*, 2nd ed.; Chapman and Hall: London, 1995. (b) Schrock, R. R.; Osborn, J. A. *Inorg. Chem.* **1970**, *9*, 2339.

(26) Kanki, K.; Misumi, Y.; Masuda, T. *Inorg. Chim. Acta* **2002**, *336*, 101.

(27) Schäfer, M.; Mahr, N.; Wolf, J.; Werner, H. *Angew. Chem., Int. Ed. Engl.* **1993**, *32*, 1315.

(28) (a) Kishimoto, Y.; Itou, M.; Miyatake, T.; Ikariya, T.; Noyori, R. *Macromolecules* **1995**, *28*, 6662. (b) Sanda, F.; Araki, H.; Masuda, T. *Macromolecules* **2005**, *38*, 10605.

(29) Synergistic effect on solvating power has also been observed in other PPA derivative systems; for example, pyrene- and ferrocene-containing PPAs show much higher solvating powers than their parent form of PPA.[4,10,30]

(30) Zhao, H.; Yuan, W. Z.; Tang, L.; Sun, J. Z.; Xu, H. P.; Qin, A.; Mao, Y.; Jin, J. K.; Tang, B. Z. *Macromolecules* **2008**, *41*, 8566.

(31) (a) Islam, M. F.; Rojas, E.; Bergey, D. M.; Johnson, A. T.; Yodh, A. G. *Nano Lett.* **2003**, *3*, 269. (b) Matarredona, O.; Rhoads, H.; Li, Z.; Harwell, J. H.; Balzano, L.; Resasco, D. E. *J. Phys. Chem. B* **2003**, *107*, 13357. (c) Yurekli, K.; Mitchell, C. A.; Krishnamoorti, R. *J. Am. Chem. Soc.* **2004**, *126*, 9902.

(32) Carrillo, A.; Swartz, J. A.; Gamba, J. M.; Kane, R. S. *Nano Lett.* **2003**, *3*, 1437.

(33) (a) *Clusters and Colloids: From Theory to Applications*; Schmid, G., Ed.; VCH: Weinheim, Germany, 1994. (b) Lewis, L. N. *Chem. Rev.* **1993**, *93*, 2693. (c) Schmid, G. *Chem. Rev.* **1992**, *92*, 1709. (d) Conway, B.; Tilak. B. In *Advances in Catalysis*; Eley, D.; Pines, H., Weisz, P., Eds.; Academic Press: New York, 1992; Vol. *38*. (e) Davis, S. C.; Klabunde, K. J. *Chem. Rev.* **1982**, *82*, 153.

(34) (a) Reetz, M. T.; Helbig, W.; Quaiser, S. A.; Stimming, U.; Breuer, N.; Vogel, R. *Science* **1995**, *267*, 367. (b) Kolb, U.; Quaiser, S. A.; Winter, M.; Reetz, M. T. *Chem. Mater.* **1996**, *8*, 1889. (c) Gallardo, I.; Pinson, J.; Vila, N. *J. Phys. Chem. B* **2006**, *110*, 19521.

(35) (a) Kerker, M. *J. Colloid Interface Sci.* **1985**, *105*, 297. (b) Magdassi, S.; Bassa, A.; Vinetsky, Y.; Kamyshny, A. *Chem. Mater.* **2003**, *15*, 2208.

MA801978X